Triple fcc-bcc-liquid point on the Xe phase diagram determined by the *N*-phase method

Anatoly B. Belonoshko*
Applied Materials Physics, Department of Material Science and Engineering, The Royal Institute of Technology, SE-10044 Stockholm, Sweden

(Received 2 March 2008; revised manuscript received 14 October 2008; published 17 November 2008)

There is a discrepancy between the fcc-bcc phase boundaries in Xe determined by the two-phase and the λ-integration methods. To resolve this issue, I performed large scale (4×10^6 atoms) molecular-dynamics simulations of fcc and bcc Xe phases embedded in liquid Xe. Such simulations, which I call *N*-phase method, allows for the hydrostatic freezing or melting and direct competition of the phases under consideration. As a result of these long (over several nanoseconds) simulations, I can place the triple fcc-bcc-liquid point on the melting curve of Xe between temperatures of 3470 and 4000 K. This suggests that certain effects are not taken into account in the previous work. Possible reasons are discussed.

DOI: 10.1103/PhysRevB.78.174109 PACS number(s): 64.70.dg

I. INTRODUCTION

A computation of phase diagram forms a basis of computational materials science. Such a computation involves two ingredients: namely, an interaction model of a material and a method to treat the model. Method, in the context of this paper, means not only a particular computational algorithm but also its particular application. Any practical realization of a method might produce certain errors that might not be intrinsic to the method as an algorithm as such but rather to its practical implementation. Ideally, when both the method and the interaction model are adequate, the computed phase diagram is reliable. Therefore, whenever a discrepancy is encountered between different methods when employing the same interaction model, it is critical to find out the reason as soon as possible. Until then, none of the methods can be trusted entirely. Such a discrepancy has recently emerged when computing phase diagram of Xe in the high-pressure (P) and high-temperature (T) ranges. High-PT phase diagram (Fig. 1) was computed first by the two-phase method[1] to explain the experimental diamond-anvil cell (DAC) data.[2] By applying an effective exp-6 pair potential and two-phase method,[3] the experimental data was explained by temperature induced transition from the face-centered-cubic (fcc) phase to the body-centered-cubic (bcc) phase. The computed diagram of Xe was substantiated further[4] by computing a number of Xe properties in very good agreement with experiment.[4] The melting curve was also computed by *ab initio* molecular-dynamics (MD) simulations.[5] The two-phase method proved to be a reliable method for calculating a melting phase boundary for a number of substances, such as $MgSiO_3$ perovskite,[3,6] Al_2O_3,[7] Fe,[8] LiF,[9] Cu,[10] H_2,[11] LiH,[12] generic Lennard-Jonesium,[13] Al,[14] MgO,[15] Pb,[16] and Mo.[17] Note that melting curves of Xe computed by the two-phase and the λ methods[18] (also known as the Ladd-Frenkel method[19]) are very close. However, application of these methods in computing the position of the triple fcc-bcc-liquid point led to completely different results. While Saija and Prestipino[18] (SP) placed that point at the temperature of about 4700 K, two-phase simulations positioned that point at about 2700 K (Fig. 1). This is a very large difference and reasons for such scatter have to be found out as well as the position of the triple point.

The Ladd-Frenkel method consists in the calculation of the Helmholtz free energy for each phase as a function of volume and temperature. From this information, a complete phase diagram can be retrieved. For the system with a given interatomic potential, it is accomplished by first choosing a system with a reference potential with the known free energy. Then, by gradually switching from the reference potential to the potential of interest and by performing the λ integration over the intermediate states, one can compute the difference of free energies between the reference system and the system of interest, and, in such a way, compute the free energies of both phases.

Before proceeding, it is important to understand what is the relationship between the two-phase and the Ladd-Frenkel methods. Both methods belong to the so-called computer experiment category so one can perform the comparison by making the parallel to a real experiment. The two-phase computer experiment is similar to the experiment where melting or solidification is observed directly. In such experiment an investigator is most often unaware of the Gibbs/Helmholtz energies of the solid and liquid phases he or she observes. Such knowledge is completely unnecessary as soon as the nature of both phases as well as the thermodynamic conditions of the transition can be reliably determined. There is yet another experimental way to determine such an equilibrium: namely, one can measure equation of state, enthalpy, heat capacities, heat of fusion, etc. for liquid and solid phases, and then, by computing the Gibbs/Helmholtz energies, determine the conditions where these energies are equal. While the two-phase method is similar to the direct observation of the transition, the Ladd-Frenkel method is similar to the latter experimental approach.

In what follows, I introduce a different method, which I call the *N*-phase method. Using this method, I showed that the statistical errors of the SP paper are too optimistic. The temperature of the bcc-fcc-liquid triple point is much lower than that provided in the SP paper. I also show that the error in SP paper is comparable to the error of the two-phase method. I present results of large scale MD simulations where all three possible phases are present. I analyzed results of these simulations and discussed the reasons for the discrepancies. I concluded by discussing the perspectives of the introduced *N*-phase method.

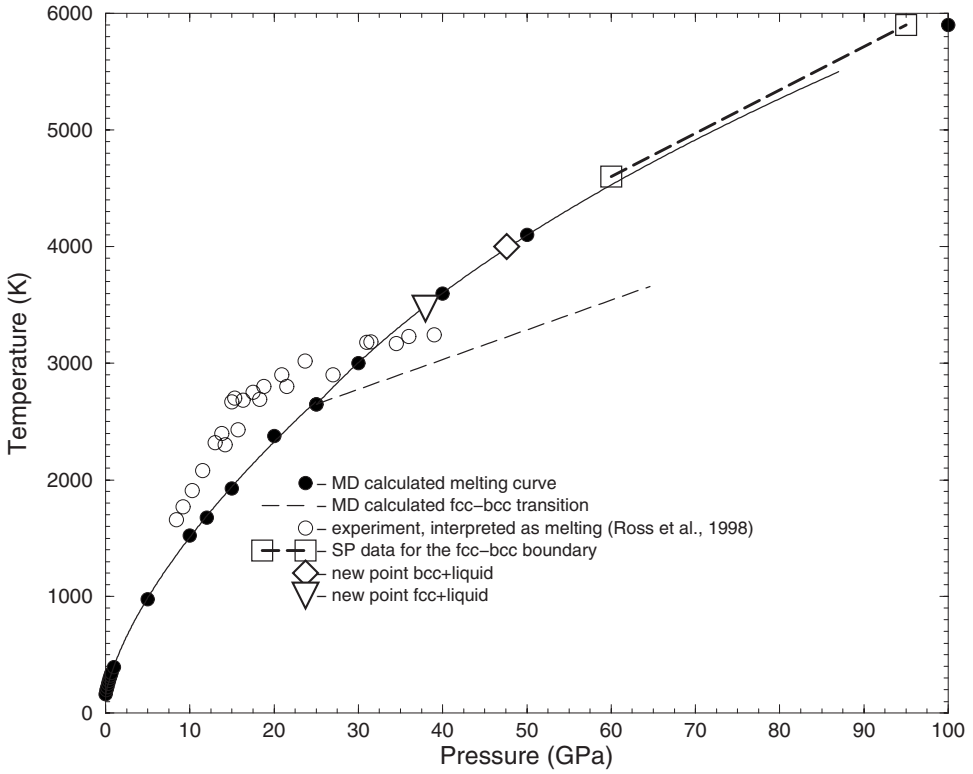

FIG. 1. MD calculated melting data (filled circles) and the fcc-bcc transition (dashed line) compared with experimental data (open circles). The MD melting data was fitted using the Simon (Ref. 4) equation in two separate ranges: from 0 to 25 GPa, and from 25 GPa up to 90 GPa. The fit is shown by solid curves. The uncertainty in determining the melting temperatures corresponds approximately to the size of filled circles. The position of the triple fcc-bcc-liquid point has uncertainty of 2.5 GPa (Ref. 4). The SP melting curve practically coincides with ours. The fcc-bcc transition, according to the SP study, is shown by the thin dashed line. The diamond symbol shows the equilibrium between bcc and liquid established in this study. The triangle shows equilibrium between bcc and liquid. The triple bcc-fcc-liquid point is located between the triangle and the diamond.

II. METHOD

A description of the molecular-dynamics method can be found elsewhere.[20] In short, the molecular-dynamics method consists of solving numerically the equations of motion for the atoms, assuming their initial coordinates and velocities, and a model for the interaction between them. Normally, as is also the case in our present MD calculations, periodic boundary conditions (PBC) are applied. PBC means that, if a particle leaves a computational cell on one side of the cell, an identical particle enters the cell from the opposite side. I performed all of the simulations using the package DL_POLY. The interaction between the atoms of Xe was described by pairwise effective potential,

$$\phi(r) = \varepsilon\left\{\frac{6}{\alpha-6}\exp\left[\alpha\left(1-\frac{r}{r^*}\right)\right]-\frac{\alpha}{\alpha-6}\left(\frac{r^*}{r}\right)^6\right\}, \quad (1)$$

where $\phi(r)$ is the energy of interaction between two atoms at a distance r. The quantities ε, r^*, and α are adjustable parameters. I used this potential [Eq. (1)] with the parameters ε/k_B=235 K, α=13.0, and r^*=4.47 Å, where k_B is the Boltzmann constant. This potential has been exhaustively studied[1,4,5] and demonstrated to perform very well. I will use metric units instead of scaled variables. Use of scaled variables is justified for two-parameter potentials. Because the parameter α is not always equal to 13,[21] use of scaled variables might be misleading.

As one can see (Fig. 1), the SP paper suggests that the bcc phase becomes stable first above 4700 K while earlier studies suggest stability already above 2700 K. To resolve this issue I decided to perform this study at pressures somewhere in between those two, namely, in the vicinity of 3400 and 4000 K. Depending on the computed phase assemblages, conclusion on the position of the triple point can be made. To find the stable phase assemblage, we need to place both bcc and fcc at the exactly same *PT* conditions and allow for the transition from one phase to another. Basically, this is what we do in a real experiment. We make an observation of the emerging structure at particular conditions. Let us make computer "experimental" observations. To that purpose I first prepare a large sample of liquid Xe. Starting from the fcc structure created as a $100\times100\times100$ multiplication of the Xe fcc unit cell with four atoms, I simulated it at pressure of 40 GPa and temperature of 6000 K, sufficiently deep in the *PT* field stability of liquid Xe (Fig. 1) to avoid complications related to superheating.[22] After that, the resulting liquid structure was equilibrated at the P=50 GPa and T =4100 K, slightly above the melting curve (Fig. 1). Thus, the liquid sample with the size $473\times473\times473$ Å^3 con-

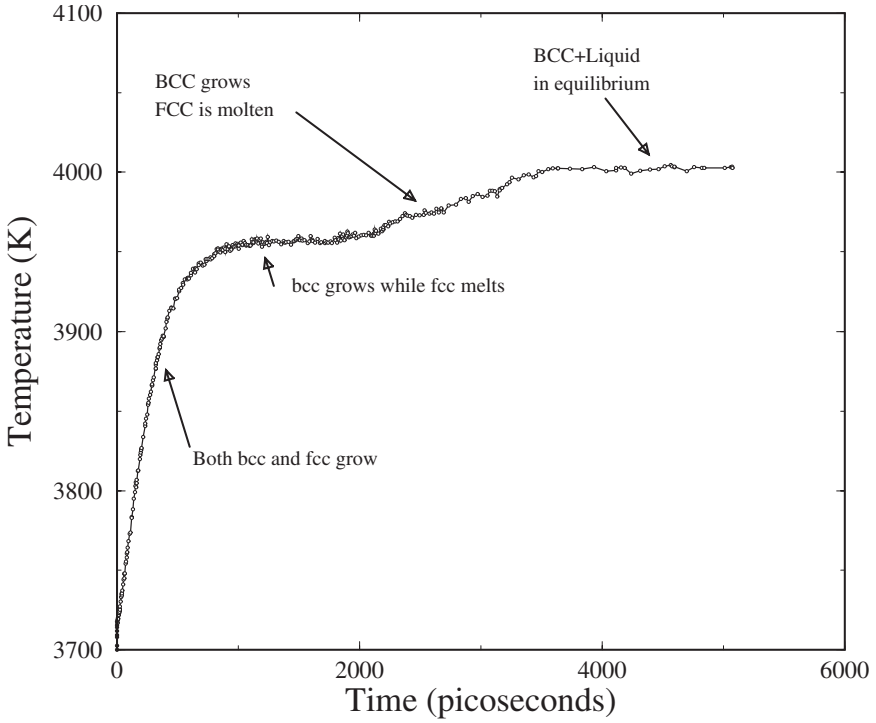

FIG. 2. Temperature during the simulation run as a function of the simulation time. The different parts of the temperature curve correspond to different processes in the simulation box, as indicated in the legend. The first stage, where the temperature of the system rapidly increases, corresponds to the growth of both bcc and fcc phases. The first flat part of the curve corresponds to the competing processes of the fcc melting and the bcc crystallization. Gradually, the amount of the crystallized bcc becomes larger than the amount of the melted fcc and the temperature goes up again. Finally, the system reaches an equilibrium. This is the state where two phases: the liquid and the bcc, are present, and their amount does not change. The resulting pressure and temperature are shown by diamond in Fig. 1.

tained 4×10^6 atoms. At the same pressure of 50 GPa but at a somewhat lower temperature of 3700 K, I simulated fcc and bcc samples. The fcc sample consisted of 256 000 atoms ($40\times40\times40$ multiplication of the unit cell with four atoms in the unit cell). Similarly, the bcc sample consisted of 250 000 atoms ($50\times50\times50$ multiplication of the unit cell with two atoms in the unit cell). That is, the sample sizes are chosen to meet two conditions. First, they have to be sufficiently large to ensure their growth. Second, they have to be of about the same size to create the conditions similar to both solid phases. These solid samples (their final MD simulated configurations) then were embedded in the box with liquid atoms. Solid samples were placed in the centers of the upper (fcc) and lower (bcc) parts of the cubic liquid sample. After the procedure of embedding and excluding liquid atoms, the total number of atoms in the box was 3984 024. After that, the system was simulated in the *NVE* (constant *N*—number of particles, *V*—volume, and *E*—energy) ensemble, where the initial temperature was set to 3700 K, about 300 K below (according to both our previous[1,4,5] and SP papers) the melting temperature. To ensure high precision and conservation of total energy, the time step was chosen to be equal to 0.5 fs. This is a very small time step considering the atomic weight of Xe (130 a.u.). After those preparations, our interference was over and we just run the simulation for several weeks accumulating the data.

III. RESULTS AND DISCUSSION

Because the initial temperature of 3700 K was substantially lower than the melting temperature (4050 K) at the initial pressure within the box (slightly lower than 50 GPa), both fcc and bcc embedded samples started to grow. In principle, the relaxation of liquid-solid interface in the initial steps of the simulation might destabilize the crystallites differently. Therefore, it is important to choose large crystallites, as is the case in this study, and to choose the initial temperature sufficiently low to ensure initial growth of both phases. The configurational energy of the solid is lower than the energy of the liquid; therefore, the released energy transforms to kinetic energy and, in turn, increases the temperature. This is reflected in the fast increase in temperature in the initial stage of the simulation (Fig. 2). There is a temperature, however, above that only one solid phase survives. One can see from Fig. 2 that this temperature is reached at about 3960 K. The analysis shows (see below) that at this temperature the fcc phase melts. Naturally, the temperature remains constant at this stage. Any temperature (=kinetic energy) overshoot is spent right away in transforming the atoms from fcc structure to liquid structure. This transition requires energy (=latent heat of melting). This energy was gained from the continuing freezing of the bcc sample. If not for bcc phase, the equilibrium would have been established at the temperature of 3960 K. As soon as the fcc phase is

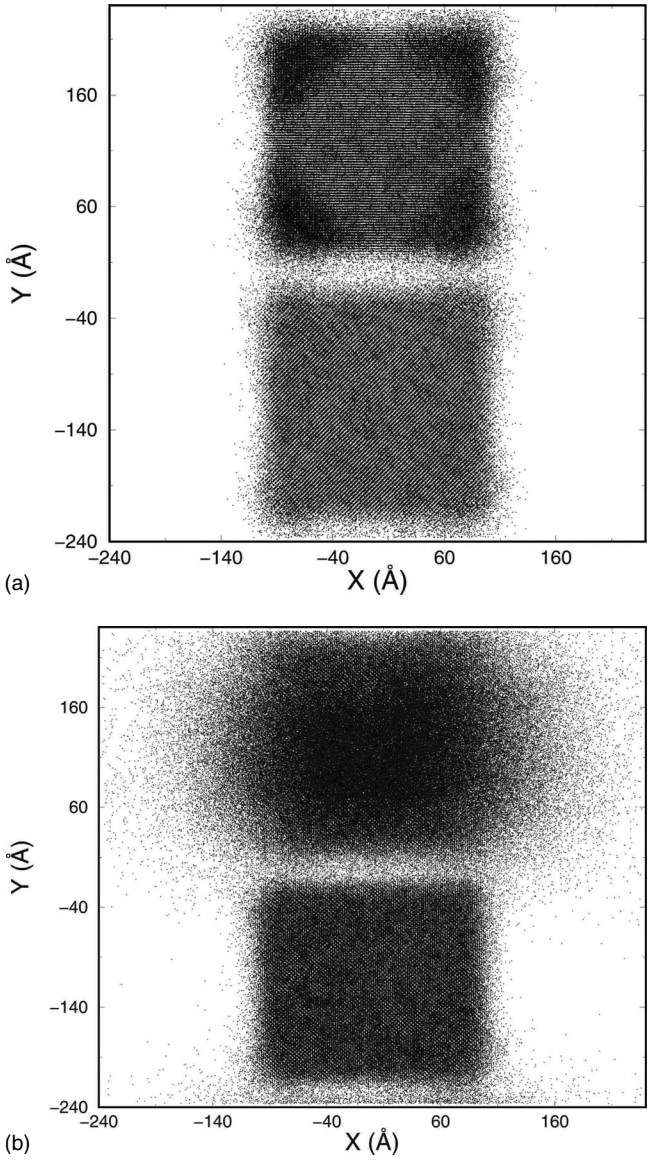

FIG. 3. *XZ* projection of the initial fcc (upper) and bcc (lower) atoms at the time of 0.1 (beginning of simulation) and 5.0 (end of simulation) ns for the simulation in Fig. 2. In the beginning both fcc and bcc parts are of the same size and, being more stable than the liquid, stay intact. At the end of the simulation, the bcc system remains intact while a substantial portion of the fcc sample has melted and diffused. Some of the initially fcc atoms remain intact because they have been captured by the growing bcc sample.

molten, the temperature rises further. Eventually, the temperature becomes constant, fluctuating around the average value of 4002.6 K. Because the crystallization decreases the pressure, it fluctuates around the value of 47.6 GPa. I want to emphasize that it is of secondary importance whether the phase that melts at lower pressure has a larger or smaller latent heat compared to the latent heat of the high-temperature phase. The equilibrium is governed by chemical potentials of the involved phases, not by their latent heats.

The question whether fcc or bcc melts at the $T=3960$ K is answered by the data provided in Figs. 3–5. Figure 3 shows projection of the fcc (upper part) and the bcc (lower part) instant configurations at different stages of simulation. Figure 3(a) shows both solid parts at the stage where both samples grow. The atoms stay intact, preserving the initial structure. The atoms, which initially belong to the liquid phase, are not shown in Fig. 3. Neither are the atoms that became a part of grown fcc or bcc samples. Figure 3(b) shows the same parts in the end of the simulation. The bcc part is not changed while the original fcc atoms spread around in the box. They do not occupy the whole box for one simple reason—it is already occupied by the enlarged bcc sample.

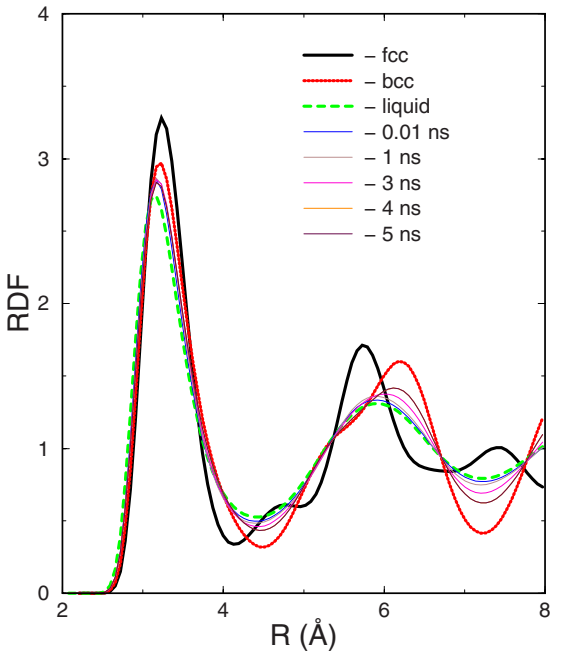

FIG. 4. (Color online) RDF of liquid, fcc, and bcc compared to RDFs of the initially three-phase (liquid, fcc, and bcc) system simulated in Fig. 2. RDFs of the system are given at a number of times as indicated on the legend. One can clearly see that the structure of the system converges toward the bcc one. The final RDF is in between the liquid and the bcc, indicating that the equilibrium state is a two-phase, liquid and bcc, system. This is in agreement with the evidence from Fig. 3.

Figure 4 is consistent with Fig. 3. Figure 4 shows radial distribution functions (RDFs) (defined as a density of probability to find an atom at a certain distance from the given atom) for liquid, fcc, and bcc Xe at the conditions of simulation. It is compared with RDFs of the system calculated at different times during the simulation. One can clearly see, particularly at the distances 6.2 and 7.3 Å, how calculated RDFs of the system converge toward the bcc structure. The final RDF at the time of 5 ns represents the RDF of the bcc and liquid mixtures.

Finally, to dismiss any wrong impressions that the atoms in the upper part of Fig. 3(b) might comprise the fcc structure, I computed the RDF for the atoms that originally belonged to the fcc crystal. To compute that RDF, I selected the atoms that were positioned within the sphere with the radius of 15 Å, where the sphere center was placed in the center of the initial fcc crystal. Then, I checked all distances between those atoms and the atoms surrounding them within the ra-

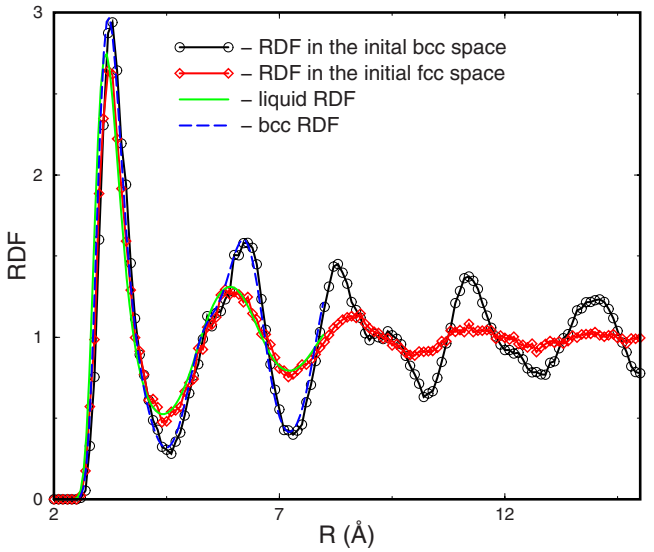

FIG. 5. (Color online) RDF computed for the atoms that comprised the bcc (solid curve with open circles) and the fcc (solid curve with diamonds) crystals in the very beginning of the MD run. These RDFs are compared with liquid RDF (solid curve without symbols) computed for the initial liquid and bcc RDF (dashed curve) computed for the initial bcc crystal. The RDF, computed for the innermost part of the initially fcc crystal, practically coincides with the liquid RDF. The RDF, computed for the innermost part of the initially bcc crystal, practically coincides with the bcc RDF. This confirms that the fcc crystal is molten while the bcc crystal preserves its structure.

dius of 15 Å. This was done for the final configuration only without averaging over configurations. However, because of the large number of atoms, the computed RDF is rather smooth (Fig. 5). Certain small fluctuations can be noted but they are of no significance. I also plotted the RDF for pure liquid (in which the original fcc crystal was immersed). One can see that the former "fcc" atoms are even less structured than the liquid. This is because of diffusion and, naturally, smaller density. However, general features of the former fcc and liquid RDFs are quite identical. This unambiguously tells us that the fcc crystal is completely molten.

In a similar way, we computed the RDF for the atoms which originally belonged to the bcc crystal. We plotted that RDF along with the RDF for the original bcc crystal that was immersed in the liquid. Again, we see that the RDFs are identical (Fig. 5). This tells us that the bcc crystal remains intact and has not molten.

In a similar way, we performed the N-phase ($N=3$) simulation at a lower pressure and temperature. Starting from the temperature of 3300 K at volume corresponding to about 38.5 GPa, we performed the simulation similar to that described above including all steps. The resulting temperature path is shown in Fig. 6. All the stages of the temperature evolution are similar to that presented in Fig. 2 with the one difference—during the first flat part of the temperature curve, unlike that in Fig. 2, it is the bcc phase that melts. Figure 7 demonstrates it very clearly. Analysis of RDFs confirms this conclusion.

Two final PT points of the bcc-liquid and fcc-liquid equilibria belong to the melting curve obtained by the two-phase

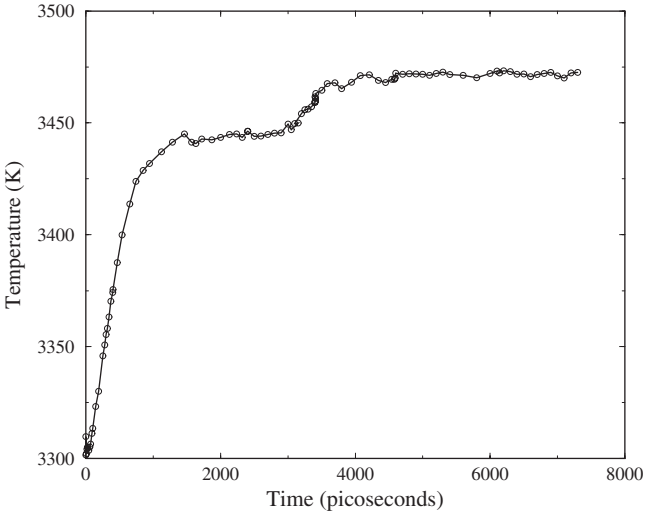

FIG. 6. Temperature during the simulation run at the density corresponding to about 40 GPa at the melting temperature (Fig. 1) as a function of simulation time. The different parts of the temperature curve correspond to different processes in the simulation box. The first stage, where the temperature of the system rapidly increases, corresponds to the growth of both bcc and fcc phases. The first flat part of the curve corresponds to the competing processes of the bcc melting and fcc crystallization. Gradually, the amount of the crystallized fcc becomes larger than the amount of the melted bcc and the temperature rises again. Finally, the system reaches an equilibrium. This is the state where two phases: liquid and fcc, are present, and their amount does not change. The resulting pressure and temperature are shown as the triangle in Fig. 1.

simulations (Fig. 1). The temperature of bcc stability is at least 700 K below the triple fcc-bcc-liquid point as calculated in the SP paper by the λ-integration technique. At the same time, it is at least 800 K higher than the triple point determined on the basis of the two-phase method. What

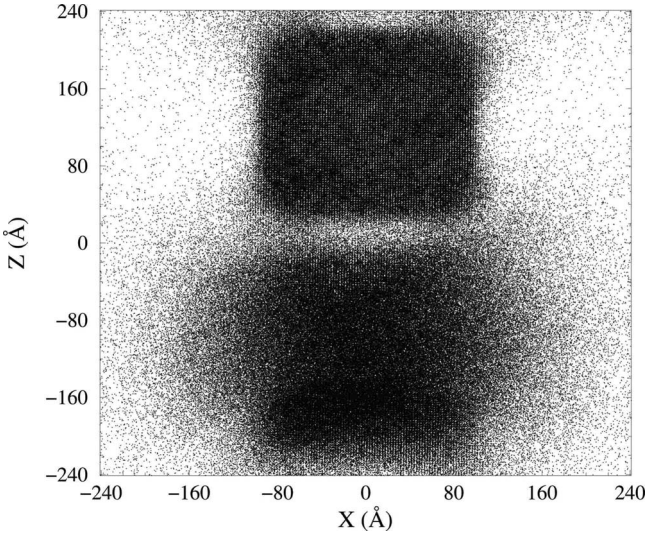

FIG. 7. XZ projection of the final positions of initially fcc (upper) and bcc (lower) atoms at the time of 7.0 ns (end of simulation) in the simulation in Fig. 6. The fcc phase remains intact while the bcc sample has melted.

could be the reason for this? First, let us discuss the SP results. One obvious reason is that the SP paper relied on the calculations of ideal samples while realistic population of defects at high temperature might be important. Note that in our simulations such a population was allowed to be established during the freezing or melting of the samples, and also by their 4 orders of magnitude larger size compared to the samples in the SP paper. Second, the size and length of SP simulations might be an issue. Finally, the approach employed by SP is a multistep procedure that accumulates errors at each stage.[14] Indeed, the authors of the SP paper wrote that their error in calculating free energies was so large that the bcc phase could already be stable within their error at the temperature of 2700 K (Fig. 1). However, Saija and Prestipino, relying on smooth behavior of their free-energy curves, dismissed such a possibility. Apparently, the error was not restricted by the smooth free-energy curves. All of the aforementioned is not to say that the λ-integration method should be abandoned. However, when energy of solid phases become very close, one has to be very careful in achieving the necessary precision.

Now, what could be the reason for the two-phase based triple point at 2700 K? When composing a two-phase cell, one has to produce an interface between liquid and solid parts of the computational cell. There is no way to know this *a priori*, and the basic assumption is that the initial exact adjustment of two parts to each other is not important. Indeed, it does allow production of a reasonable melting curve. However, when two solid phases are energetically close to each other, such adjustment might create certain possibilities for destabilizing the solid part of the two-phase cell, and this destabilization might be sufficient in transforming one phase to another. Perhaps, when placing together fcc and liquid, some space was left between the two parts and this locally allowed the decrease in the pressure and, in this way, destabilize the fcc phase in favor of bcc phase. This could only be possible due to rather small number of atoms in the two-phase simulations. Also, the transformation from the two-phase fcc-liquid assemblage into single bcc phase during two-phase simulation occurred from the very beginning of the simulation. In the presented *N*-phase simulations, it was ensured that both phases initially grew; therefore the transient character of the transition was excluded, unlike to two-phase simulations.

Finally, the simulations in this paper were performed with much larger number of atoms than in previous works.[1,18] It was observed that the periodic boundary conditions might affect properties of solid phases when the number of particles is low[23] because of neglecting of the long phonons. It could be that such neglect affected the SP results and erroneously stabilized the fcc phase up to much higher *PT* conditions. The impact of small size is likely to be larger on the SP results because the two-phase simulations were performed for much larger systems than the SP simulations.

The exact position of the triple point remains to be determined by additional *N*-phase simulations. However, this is hardly needed. As one can see from Figs. 2 and 6, the differences between melting temperatures of two solid phases on each figure are close to each other (being somewhat smaller in Fig. 6). Therefore, the triple point can be, with reasonable precision, positioned at about 3700 K. This is basically in the middle between 2700 (Ref. 1) and 4700 K (Ref. 18) (Fig. 1). I call the approach in this paper the *N*-phase method because it is not restricted to the number of phases. One can place all solid phases in the box with the liquid of the same composition and in one run, although long, determine the stability of the most stable high-*PT* phase. It is not impossible that even a new phase might grow at a surface of one of the solid phases.

IV. CONCLUSIONS

I have suggested a method (*N* phase) in choosing the most stable solid phase on heating. Unlike the coexistence[13] method, the *N*-phase method is free from nonhydrostatic stress. It is not restricted by any number of involved phases. While λ method has never been applied to anything more complex than a monatomic substance, the introduced *N* method can be applied, similar to the two-phase method,[3] to substances of any chemical and structural complexity. In a single run, it allows solving of the problem of finding the most stable phase. Applying this method, I demonstrated that the position of the Xe bcc-fcc-liquid point has to be moved to about 3700 K on the melting curve (Fig. 1).

ACKNOWLEDGMENTS

Computations were performed at the National Supercomputer Center in Linköping, at the Parallel Computer Center in Stockholm, and at the Los Alamos National Laboratory (Los Alamos, New Mexico). I also thank the Swedish Research Council (VR) and the Swedish Foundation for Strategic Research (SSF) for financial support.

*anatoly@fysik.uu.se

[1] A. B. Belonoshko, R. Ahuja, and B. Johansson, Phys. Rev. Lett. **87**, 165505 (2001); **89**, 119602 (2002).

[2] R. Boehler, M. Ross, P. Soderlind, and D. B. Boercker, Phys. Rev. Lett. **86**, 5731 (2001).

[3] A. B. Belonoshko, Geochim. Cosmochim. Acta **58**, 4039 (1994).

[4] A. B. Belonoshko, O. LeBacq, R. Ahuja, and B. Johansson, J. Chem. Phys. **117**, 7233 (2002).

[5] A. B. Belonoshko, S. Davis, A. Rosengren, R. Ahuja, B. Johansson, S. I. Simak, L. Burakovsky, and D. L. Preston, Phys. Rev. B **74**, 054114 (2006).

[6] A. B. Belonoshko, N. V. Skorodumova, A. Rosengren, R. Ahuja, B. Johansson, L. Burakovsky, and D. L. Preston, Phys. Rev. Lett. **94**, 195701 (2005).

[7] A. B. Belonoshko, Phys. Chem. Miner. **25**, 138 (1998); R. Ahuja, A. B. Belonoshko, and B. Johansson, Phys. Rev. E **57**,

1673 (1998).
[8] A. B. Belonoshko and R. Ahuja, Phys. Earth Planet. Inter. **102**, 171 (1997); A. B. Belonoshko, R. Ahuja, and B. Johansson, Phys. Rev. Lett. **84**, 3638 (2000); Nature (London) **424**, 1032 (2003).
[9] A. B. Belonoshko, R. Ahuja, and B. Johansson, Phys. Rev. B **61**, 11928 (2000).
[10] A. B. Belonoshko, R. Ahuja, O. Eriksson, and B. Johansson, Phys. Rev. B **61**, 3838 (2000); L. Vocadlo, D. Alfè, G. D. Price, and M. J. Gillan, J. Chem. Phys. **120**, 2872 (2004).
[11] S. Bonev, E. Schwegler, T. Ogitsu, and G. Galli, Nature (London) **431**, 669 (2004).
[12] T. Ogitsu, E. Schwegler, F. Gygi, and G. Galli, Phys. Rev. Lett. **91**, 175502 (2003).
[13] A. J. C. Ladd and L. V. Woodcock, Chem. Phys. Lett. **51**, 155 (1977).
[14] J. R. Morris, C. Z. Wang, K. M. Ho, and C. T. Chan, Phys. Rev. B **49**, 3109 (1994); B. J. Jesson and P. A. Madden, J. Chem. Phys. **113**, 5924 (2000).
[15] A. B. Belonoshko and L. Dubrovinsky, Am. Mineral. **81**, 303 (1996); A. Strachan, T. Cagin, and W. A. Goddard, Phys. Rev. B **63**, 096102 (2001); A. B. Belonoshko, *ibid.* **63**, 096101 (2001); A. Aguado and P. A. Madden, Phys. Rev. Lett. **94**, 068501 (2005); D. Alfè, *ibid.* **94**, 235701 (2005).
[16] F. Cricchio, A. B. Belonoshko, L. Burakovsky, D. L. Preston, and R. Ahuja, Phys. Rev. B **73**, 140103(R) (2006).
[17] C. Cazorla, M. J. Gillan, S. Taioli, and D. Alfè, J. Chem. Phys. **126**, 194502 (2007).
[18] F. Saija and S. Prestipino, Phys. Rev. B **72**, 024113 (2005).
[19] D. Frenkel and A. J. C. Ladd, J. Chem. Phys. **81**, 3188 (1984).
[20] M. P. Allen and D. J. Tildesley, *Computer Simulation of Liquids* (Clarendon, Oxford, 1987).
[21] A. B. Belonoshko and S. K. Saxena, Geochim. Cosmochim. Acta **55**, 381 (1991); **55**, 3191 (1991).
[22] A. B. Belonoshko, N. V. Skorodumova, A. Rosengren, and B. Johansson, Phys. Rev. B **73**, 012201 (2006); A. B. Belonoshko, S. Davis, N. V. Skorodumova, P. H. Lundow, A. Rosengren, and B. Johansson, *ibid.* **76**, 064121 (2007).
[23] A. Aguado, L. Bernasconi, and P. A. Madden, Chem. Phys. Lett. **356**, 437 (2002).